Available online at www.sciencedirect.com
ScienceDirect
Journal of Organometallic Chemistry 692 (2007) 3778–3787
Journal of Organometallic Chemistry
www.elsevier.com/locate/jorganchem

Theoretical study of the two-photon absorption properties of octupolar complexes with Cu(I), Zn(II) and Al(III) as centers and bis-cinnamaldimine as ligands

Xiang-Biao Zhang [a], Ji-Kang Feng [a,b,*], Ai-Min Ren [a]

[a] State Key Laboratory of Theoretical and Computational Chemistry, Institute of Theoretical Chemistry, Jilin University, Changchun 130023, People's Republic of China
[b] College of Chemistry, Jilin University, Changchun 130023, People's Republic of China

Received 19 December 2006; received in revised form 3 March 2007; accepted 6 March 2007
Available online 21 March 2007

Abstract

The equilibrium geometries, electronic structures, one- and two-photon absorption (TPA) properties of a series of octupolar complexes with the Cu(I), Zn(II) and Al(III) as coordinate centers and the bis-cinnamaldimine as ligands have been studied using the B3LYP/6-31G(d) and ZINDO-SOS methods. Compared with the dipolar metal complexes, all the octupolar metal complexes (including tetrahedral and octahedral complexes) have relatively large TPA cross-sections, indicating that building octupolar metal complex is an effective route to design of promising TPA material. Lewis acidity of metal center and molecular symmetry are two important factors for enhancement of TPA cross-section of metal complex. Due to the stronger Lewis acidity of Zn(II) than Cu(I) as well as Al(III) than Zn(II), the tetrahedral Zn(II) complex exhibits a TPA cross-section larger than that of the tetrahedral Cu(I) complex, the maximum TPA position of the octahedral Al(III) complex is red-shifted relative to the octahedral Zn(II) complex, and at the same time, the octahedral Al(III) complex has a large TPA cross-section. Compared with the tetrahedral complexes, the TPA cross-sections of the octahedral complexes are enhanced due to the increased number of ligands.

Keywords: Two-photon absorption; Octupolar metal complexes; ZINDO-SOS method

1. Introduction

Two-photon absorption (TPA) in molecule has received considerable attention in recent years, owing to a number of potential applications [1–4] in several areas of bio-photonics and material science, such as two-photon up-conversion lasing [1], optical power limiting [2], photodynamic therapy [3], and three-dimensional (3D) microfabrication [4]. The push–pull dipolar molecules, in the earlier studies, have been the active research point, because this kind of molecules generally has large TPA cross-sections [5–10]. However, these dipoles may present many problems from a material standpoint [11], and it is the dipole–dipole electrostatic interactions that often result in an antiparallel molecular arrangement and a subsequent cancellation of the nonlinear response at bulk materials. In addition, the optimized molecular structures for this kind of molecules often lead to red-shift of linear absorption, damaging the transparency of materials. In order to overcome these difficulties, the enlarged potential for nonlinear optics of octupolar molecules [12,13] has sparked intense research in design of excellent TPA materials. Compared with the 1D dipolar TPA chromophores, octupolar molecules possess more round-off shapes, which ease their packing in a single crystalline lattice as opposed to less favorable elongated dipolar rodlike molecules; the absence of dipolar moments in excited as well as ground state makes

* Corresponding author. Address: College of Chemistry, Jilin University, Changchun 130023, People's Republic of China. Tel.: +86 431 8499856; fax: +86 431 8945942.
E-mail address: jikangf@yahoo.com (J.-K. Feng).

0022-328X/$ - see front matter © 2007 Elsevier B.V. All rights reserved.
doi:10.1016/j.jorganchem.2007.03.021

octupolar molecules more suitable in various optical applications [14–16]. More importantly, octupolar compounds resolve the inherent conflict between the transparency and nonlinearity existing in traditional dipolar molecules. The results of experiments and theoretical calculations reveal that the TPA cross-section value increases on proceeding from dipolar to octupolar molecules and also with increasing donor and acceptor strength [17–21]. Most octupolar systems developed to date are organic molecules. They have been designed by chemical functionalization of a central core and can be roughly classified into three main classes: (1) 2D or 3D molecules of global D_{3h} and C_3 symmetry obtained by 1,3,5-functionalization of a central aromatic core (phenyl, or triazine) [19]; (2) D_{3h} or slightly twisted D_3 propeller-like molecules, such as functionalized trivalent carbocation, boron, aluminum or nitrogen atoms [20]; and (3) 3D tetrahedral molecules, such as tetrasubstituted carbon or phosphonium derivatives [21a]. Other examples of octupolar structures, such as paracyclophane, truxenone, sumanene and triphenylene derivatives, have also been described recently [21b–e].

Coordination chemistry has been proved to be another powerful tool to build up octupolar arrangements. Metal ions can assemble organic ligands in a variety of multipolar arrangements which show interesting electronic and optical properties tunable by virtue of the coordinated metal center. In the UV–Vis region of spectrum of metal complexes, there are often two different transitions, i.e., a strong intraligand charge-transfer (ILCT) transition and a low-energy metal to ligand charge-transfer transition (MLCT), which are often associated with large TPA cross-section. High damage threshold and fast response time that metal complexes have in comparison to organic compounds are important from the perspective of application. A wide range of metals with different oxidation states and ligands necessarily make metal complexes active research point in design of TPA material. Some reports are available describing the effect of metal ions on TPA-active organic molecules. Metal cation Mg(II) was shown to lower the TPA cross-section values by 50% in an azo-crown ether connected to distyrylbenzenes in the donor-π–acceptor-π-donor format [22]. Upon binding with Ni(II) ion, the TPA cross-sections of 1,10-phenanthroline-based π-conjugated TPA chromophores increase from 165 GM (1 GM = 10^{-50} cm^4 s/photon) to 578 GM [23]. Recently, Debabrata and Parimal et al. point out that complexation of the bis-cinnamaldimine (**L**) with metal cation can enhance electron-withdrawing character of the central diimine, making the complexes potential candidates for third-order nonlinear responses [24].

In this paper, we design octupolar complexes $\mathbf{ML_2}$ ($\mathbf{M}$ = Cu(I), Zn(II)) and $\mathbf{ML_3}$ ($\mathbf{M}$ = Zn(II) and Al(III)), study their equilibrium geometries and electronic structures with the B3LYP density functional combined with 6-31G(d) basis set, and calculate their one-photon absorption (OPA) and TPA properties using ZINDO-SOS method. Our aim is to theoretically study effects of the different symmetry of molecule and cationic center on the geometries, OPA and TPA properties of octupolar metal complexes with the bis-cinnamaldimine ligands.

2. Theoretical methodology

The TPA process corresponds to simultaneous absorption of two photons. The TPA efficiency of an organic molecule, at optical frequency $\omega/2\pi$, can be characterized by the TPA cross-section $\delta(\omega)$. It can be directly related to the imaginary part of the second hyperpolarizability $\gamma(-\omega;\omega,\omega,-\omega)$ by [25,26]

$$\delta(\omega) = \frac{3\hbar\omega^2}{2n^2c^2\varepsilon_0} L^4 \mathrm{Im}[\gamma(-\omega;\omega,-\omega,\omega)] \tag{1}$$

where $\hbar\omega$ the energy of incoming photons, c the speed of light, and ε_0 the vacuum electric permittivity. n denotes the refractive index of medium and L corresponds to the local-field factor. In the calculations presented here, n, L are set to 1 (isolated molecule in vacuum).

The sum-over-states (SOS) expression to evaluate the components of the second hyperpolarizability $\gamma_{\alpha\beta\gamma\delta}$ can be derived using perturbation theory. By considering a power expansion of energy with respect to the applied field, the methodology adopted here to calculate the second hyperpolarizability is given in the form shown in the literatures [27,28]. In the present work, all damping factors Γ are set 0.1 eV. To compare the calculated δ value with experimental value measured in solution, the orientationally averaged (isotropic) value of γ is evaluated, which is defined as:

$$\langle\gamma\rangle = \frac{1}{15}\sum_{i,j}(\gamma_{iijj} + \gamma_{ijij} + \gamma_{ijji}) \quad i,j = x,y,z \tag{2}$$

Substituted the imaginary part of $\langle\gamma\rangle$ into the expression (1), $\delta(\omega)$ that can be compared with the experimental value is obtained.

Generally, for centrosymmetric molecules, the position and relative strength of the two-photon response can be roughly predicted using the following simplified form of the SOS expression [20c]:

$$\delta \propto \frac{M_{0k}^2 M_{kn}^2}{(E_{0k} - E_{0n}/2)^2 \Gamma} \tag{3}$$

where M_{0k} and M_{kn} denote the transition dipole moment from state 0 to k and the transition dipole moment from state k to n, respectively; E_{0k} and E_{0n} denote the excitation energies from state 0 to k as well as 0 to n, respectively; the subscripts 0, k, and n refer to the ground state S_0, the intermediate state S_k, and the TPA final state S_n, respectively.

In this paper, the DFT/B3LYP/6-31G(d) method was firstly used to calculate molecular equilibrium geometries using the GAUSSIAN 03 program suite [29]. Then the property of electronic excited state was obtained by the single and double electronic excitation configuration interaction (SDCI) using the ZINDO program [30]. For all the molecules studied here, the Mataga–Nishimoto potential was employed to describe long-range Coulomb interactions;

the CI-active spaces were restricted to the 15 highest occupied and fifteen lowest unoccupied π-orbitals for singly excited configuration and to the three highest occupied and three lowest unoccupied π-orbitals for doubly excited configuration. Furthermore, the UV–Vis (the ground-state one-photon absorption) spectra which are needed to predict the TPA properties of molecule were provided. Finally, according to the formula (1) and (2) as well as the sum-over-state (SOS) expression, the second hyperpolarizability γ and TPA cross-section $\delta(\omega)$ were calculated. The calculated TPA cross-section of every molecule includes the contributions from 200 lowest-lying excited states.

3. Results and discussion

3.1. Molecular design and geometry optimization

The investigated metal complexes are shown in Fig. 1. By combination of two or three Schiff base ligands **L** with Zn(II), the tetrahedral and octahedral complexes **2-Zn** and **3-Zn** are formed, respectively. In order to comparatively study, the Zn(II) centers of **2-Zn** and **3-Zn** are replaced by Cu(I) and Al(III), respectively, forming the metal complexes **2-Cu** and **3-Al**. The ligand bis-cinnamaldimine **L** and the dipole metal complexes CuCl(L) (**1-Cu**) and $ZnCl_2$(L) (**1-Zn**) are also calculated together.

All the studied molecules are optimized using the B3LYP density functional combined with 6-31G(d) basis set. Selected bond lengths and bond angles are tabulated in Table 1 (see Scheme 1 for the labels). Complexation of **L** with metal cation increases the double bonds C_1=C_2 and C_3=N_1 lengths and reduces the C_2–C_3 bond length, indicating the ligands in metal complex are more strongly polarized dipole unit. On going from **2-Zn** to **3-Zn**, the Zn–N bond length increases (2.000 Å for **2-Zn** vs. 2.233 Å for **3-Zn**, respectively), due to the increased number of ligand in compound **3-Zn**. The Al–N bond length in **3-Al** (2.074 Å) is shorter than the Zn–N bond length in **3-Zn** (2.233 Å), due to the different cationic radii of Al(III) and Zn(II) (0.51 Å for Al(III) and 0.74 Å for Zn(II), respectively). Dipole molecules **L**, **1-Cu** and **1-Zn** are Cs symmetry, while molecules **2-Cu** and **2-Zn** show D_{2d} symmetry and molecules **3-Zn** and **3-Al** are D_3 symmetry. Taking molecules **1-Zn**, **2-Zn** and **3-Zn** as examples, their optimized space-filling geometries are shown in Fig. 2.

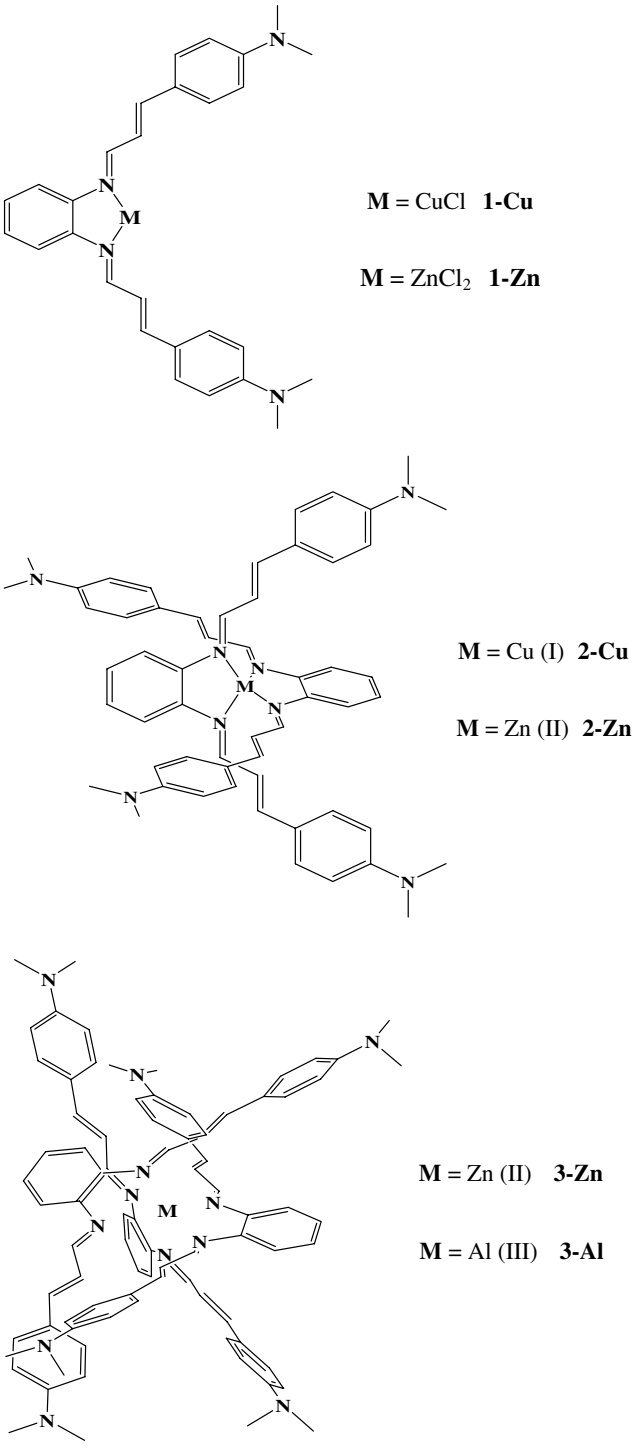

Fig. 1. Structures of studied complexes.

3.2. Electronic structures

The predicted frontier orbital energies of studied molecules are schematically plotted in Fig. 3 and the contours of the highest occupied molecular orbitals (HOMO) and the lowest unoccupied molecular orbitals (LUMO) are plotted in Fig. 4. From Fig. 3, it can be found that complexation of **L** with metal cation lowers the HOMO (except **1-Cu**) and LUMO energies, leading to reduction of the HOMO–LUMO gaps. At the level of B3LYP/6-31g(d) method, the HOMO energy of **1-Cu** is increased by 0.74 eV relative to ligand **L**. The HOMO–LUMO energy gaps of **L**, **1-Cu** and **1-Zn** are 3.32 eV, 2.11 eV and 2.82 eV, respectively. Comparing the HOMOs and LUMOs of **2-Cu** and **2-Zn**, it can be found that the HOMO and LUMO energies in **2-Zn** are decreased by 2.55 eV and 2.30 eV relative to **2-Cu**, respectively. The energy gap between the HOMO and LUMO in **2-Zn** is increased by 0.25 eV relative to **2-Cu**. The HOMO and LUMO energies

Table 1
Selected calculated bond lengths in Å and bond angles in °

Mol.	L	1-Cu	1-Zn	2-Cu	2-Zn	3-Zn	3-Al
C_1–C_2	1.355	1.361	1.363	1.366	1.379	1.372	1.385
C_2–C_3	1.445	1.426	1.424	1.424	1.410	1.420	1.405
C_3–N_1	1.287	1.309	1.303	1.309	1.318	1.315	1.333
N_1–C_4	1.398	1.403	1.405	1.413	1.414	1.411	1.416
N_1–M		1.935	2.074	1.995	2.000	2.233	2.074
N_2–M–N_1		85.0	79.8	84.3	85.1	77.2	81.7
M–N_1–C_4		110.9	110.0	111.6	110.6	112.4	111.8
M–N_1–C_4–C_5		−11.7	−20.0	0.0	0.0	0.6	0.8
C_3–N_1–C_4–C_5	138.75	148.4	158.7	180.0	180.0	−159.8	−162.7

of octahedral complex **3-Zn** (−8.03 eV and −5.56 eV, respectively) are larger than that of **2-Zn** (−8.65 eV and −6.15 eV, respectively), while the HOMO–LUMO energy gap in **3-Zn** (2.47 eV) is smaller than that in **2-Zn** (2.50 eV). Compared with tetrahedral complex **2-Zn**, the energy levels of the frontier orbitals in octahedral **3-Zn** are closer each other in energies. Replacing Zn(II) in **3-Zn** by Al(III) causes decrease of the HOMO and LUMO energies as well as the reduction the HOMO–LUMO energy gap. The HOMO and LUMO energies in octahedral complex **3-Al** as well as the energy gap between them are −9.87 eV, −7.62 eV and 2.25 eV, respectively. In the energy diagram, an obvious characteristic is that the LUMO + 1 and LUMO + 2 in dipolar molecules **L**, **1-Cu** and **1-Zn** as well as the LUMO + 3 and LUMO + 4 in tetrahedral complexes **2-Cu** and **2-Zn** are all separated by a comparatively large energy gap. The energy gaps between LUMO + 1 and LUMO + 2 in the dipolar molecules **L**, **1-Cu** and **1-Zn** are 1.30 eV, 1.71 eV and 1.71 eV, respectively, while the energy gaps between LUMO + 3 and LUMO + 4 in the tetrahedral complexes **2-Cu** and **2-Zn** are 1.59 eV and 1.85 eV, respectively. According to the symmetry of molecule and the calculated energy, the HOMO and HOMO − 1 in **2-Cu** and **2-Zn** as well as the HOMO − 1 and HOMO − 2, and the LUMO + 1 and LUMO + 2 in **3-Zn** and **3-Al** are degenerate each other. As shown in Fig. 4, the HOMOs in **L**, **1-Zn**, **3-Zn** and **3-Al** are mainly distributed on the peripheries and phenylene ring, the electron clouds of HOMO in copper (I) complexes **1-Cu** and **2-Cu** are mainly positioned on the metal center Cu^+, and for **2-Cu**, there are large contributions on the peripheries of molecule, while the LUMOs in all the molecules are mainly localized on the diimine moiety. Therefore, during one electron excitation from the HOMO to LUMO, there is the ILCT for **L**, **1-Zn**, **3-Zn** and **3-Al**, the MLCT for **1-Cu**, and the both MLCT and ILCT for **2-Cu**. This is correlated to the Lewis acidity of metal cation: Al(III) > Zn(II) > Cu(I). The different electronic transition nature will lead to the different OPA and TPA properties.

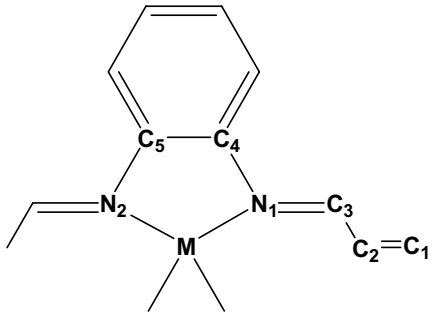

Scheme 1. Atomic labels for investigated molecules.

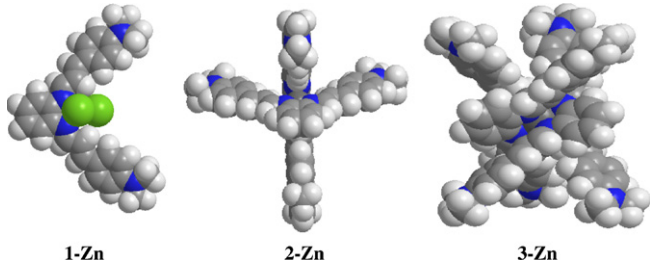

Fig. 2. Space-filling diagram for tetrahedral complex **2-Zn** and octahedral complex **3-Zn**.

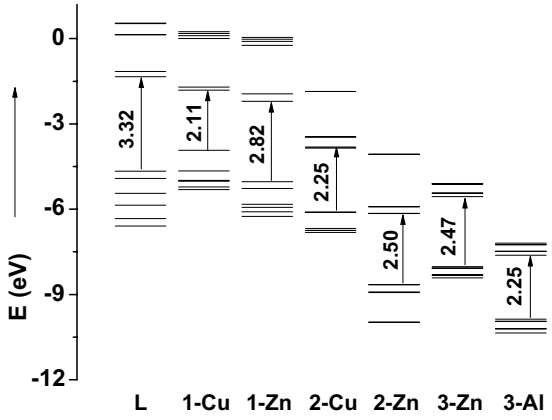

Fig. 3. The schematically plotted molecular orbitals and the energy gaps (in eV) between HOMO and LUMO.

3.3. One-photon absorptions

Table 2 lists the calculated and experimental (given in parentheses) OPA wavelengths λ_{one}, which correspond to the main one-photon absorptions, the corresponding oscillator strengths f^{cal} as well as the nature of transition for studied molecules. Because the experiment was carried

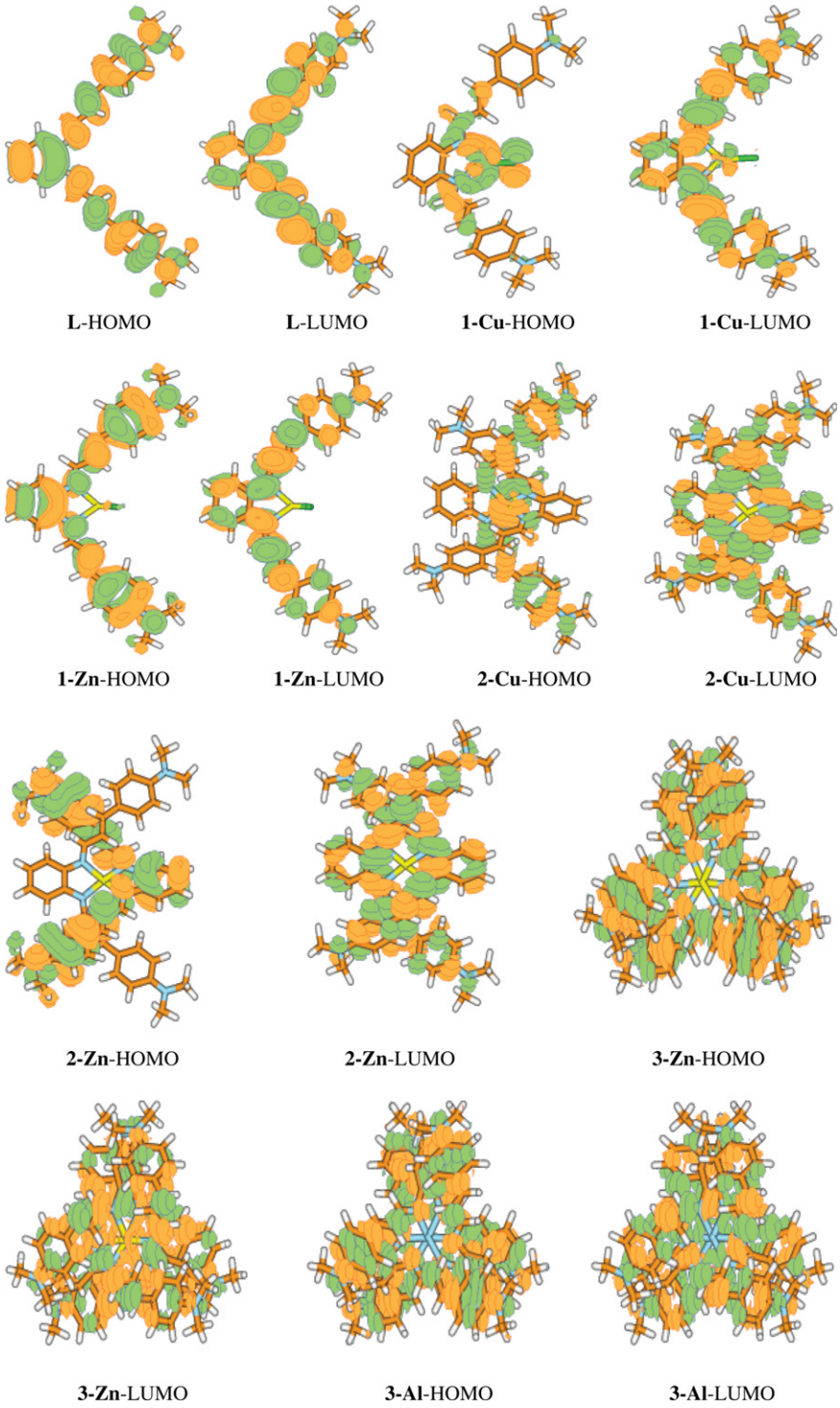

Fig. 4. Contour surfaces of HOMO and LUMO orbitals for studied molecules.

out in the dichloromethane solvent, while our calculations were curried out in the vacuum medium, the appropriate deviations between the calculated results and experimental observations are understandable. Our calculated results are generally in agreement with the experimental values.

The calculated maximum OPA wavelengths of the free ligand **L** and the dipolar metal complexes **1-Cu** and **1-Zn** are 408.7 nm, 458.0 nm and 485.0 nm, respectively. Apparently, complexation of ligand **L** with metal cation causes the red-shift of the maximum OPA. Compared with the ligand **L**, the OPA wavelengths for metal complexes **1-Cu** and **1-Zn** are red-shifted by 49.3 nm and 76.3 nm, respectively. On going from the dipolar complexes **1-Cu** and **1-Zn** to the tetrahedral complexes **2-Cu** and **2-Zn**, the maximum OPAs are further red-shifted (504.0 nm for **2-Cu** vs. 458.0 nm for **1-Cu**; 564.1 nm for **2-Zn** vs. 485.0 nm for

Table 2
The calculated one-photon absorptions properties and the available experimental values (in the parentheses)

Mol.	Transitions	λ_{one}^{cal} (λ_{one}^{exp}) nm	f^{cal}
L	$S_0 \rightarrow S_1$	408.7	0.849
	$S_0 \rightarrow S_2$	382.4 (378)[a]	0.481
1-Cu	$S_0 \rightarrow S_1$	511.1	0.452
	$S_0 \rightarrow S_3$	458.0	0.665
	$S_0 \rightarrow S_4$	413.3	1.048
1-Zn	$S_0 \rightarrow S_1$	485.0 (494)[b]	1.170
	$S_0 \rightarrow S_2$	423.6 (448)[a]	1.109
2-Cu	$S_0 \rightarrow S_1$	504.0	1.358
	$S_0 \rightarrow S_2$	504.0	1.358
	$S_0 \rightarrow S_5$	450.5 (461)[a]	1.199
2-Zn	$S_0 \rightarrow S_1$	564.1 (550)[b]	1.387
	$S_0 \rightarrow S_2$	564.1	1.387
	$S_0 \rightarrow S_3$	492.8 (493)[a]	1.993
3-Zn	$S_0 \rightarrow S_1$	536.9	0.802
	$S_0 \rightarrow S_2$	536.9	0.802
	$S_0 \rightarrow S_3$	519.2	2.864
	$S_0 \rightarrow S_4$	475.8	1.012
	$S_0 \rightarrow S_5$	475.8	1.012
3-Al	$S_0 \rightarrow S_1$	609.0	0.927
	$S_0 \rightarrow S_2$	609.0	0.927
	$S_0 \rightarrow S_3$	582.6	3.248
	$S_0 \rightarrow S_4$	544.2	0.709
	$S_0 \rightarrow S_5$	544.2	0.709

[a] Measured in dichloromethane solvent, Ref. [24].
[b] Evaluated from Figure S2 in Supporting Information, Ref. [24].

1-Zn). As the number of coordinated ligands further increases, the maximum OPA of the octahedral complex **3-Zn** is blue-shifted by 27.2 nm relative to the tetrahedral complex **2-Zn** (536.9 nm for **3-Zn** vs. 564.1 nm for **2-Zn**, respectively). Due to replacing the Zn(II) in **3-Zn** by Al(III), the maximum OPA of **3-Al** is red-shifted by 72.1 nm (609.0 nm for **3-Al** vs. 536.9 nm for **3-Zn**, respectively).

Comparing the one-photon absorptions of two tetrahedral complexes **2-Cu** and **2-Zn**, it can be found that the OPA of **2-Zn** is red-shifted by 60.1 nm relative to **2-Cu** (564.1 nm for **2-Zn** vs. 504.0 nm for **2-Cu**, respectively). Their absorptions mainly come from one electron excitation from the HOMO to LUMO. From the discussion in Section 3.2, we know that during one electron excitation from the HOMO to LUMO, there are the MLCT and ILCT for **2-Cu**, while for **2-Zn**, there is only the ILCT. Therefore, the increased ILCT in **2-Zn** relative to **2-Cu** is a main reason for redshift of one-photon absorption.

Compared to the octahedral complex **3-Zn**, the one-photon absorption of the tetrahedral complex **2-Zn** exhibits a redshift ($\Delta\lambda = 27$ nm). There is a spiroconjugation effect [31] in the tetrahedral complex **2-Zn**, while in the octahedral metal complex **3-Zn**, due to the more ligands, the **Zn–N** is lengthened relative to **2-Zn** (2.233 nm vs. 2.000 nm, respectively), and the coupling effect among the ligands is little. In addition, in the complex **2-Zn**, the dihedral angle C_3–N_1–C_4–C_5 is 180°, indicating that the Schiff base ligands in **2-Zn** are planar, while in the complex **3-Zn**, the dihedral angle C_3–N_1–C_4–C_5 is −159.8°, so diaminophenyl-vinyl plane is twisted about 20° from the phenylene ring in the Schiff base ligands in **3-Zn**. Compared to the twisted structures of the ligands in **3-Zn**, the planar structures of the Schiff base ligands in **2-Zn** favor π-electron conjugation. In the previous study, the one-photon absorption of the tetrahedral Zn(II) complex with bipyridyl ligand exhibits a larger redshift ($\Delta\lambda = 107$ nm) relative to the octahedral Zn(II) bipyridine complex [32]. This larger redshift is attributed to the strong spiroconjugation effect in the tetrahedral Zn(II) bipyridine complex. Apparently, compared with the tetrahedral Zn(II) bipyridine complex, the spiroconjugation effect in the tetrahedral Zn(II) complex with the bis-cinnamaldimine ligands is comparatively weak.

3.4. Two-photon absorptions

According to the expressions (1) and (2) and SOS formula, we calculate the third-order optical susceptibilities γ and the TPA cross-sections $\delta(\omega)$ of studied molecules. This method is extensively employed to calculation on TPA properties of many systems and proved to be reliable [5,20c,33]. The drawing of TPA energy $\lambda^{(T)}$ vs. TPA cross-section $\delta(\omega)$ of every molecule is plotted in Fig. 5. Table 3 summarizes the position of the maximum TPA ($\lambda_{max}{}^{T}$) and the nature of transition for every molecule. As shown in Table 3, though the calculated TPA wavelengths $\lambda^{(T)}$ are blue-shifted relative to the experimental observations, our calculated results are reminiscent of the change tendency of the experimentally measured TPA cross-sections. The calculated cross-section values of the TPA peak I for **1-Zn**, peak II for **2-Cu** and peak I for **2-Zn** are 2202.5 GM, 9488.8 GM and 10015.2 GM, respectively, while the corresponding experimental values of **1-Zn**, **2-Cu**, and **2-Zn** are 1769 GM, 10198 GM, and 10736 GM, respectively. Therefore, relative error of the calculated TPA cross-section for **1-Zn** is 24.5%, while relative errors of the calculated TPA cross-sections for **2-Cu** and **2-Zn** are within 10%. Metal complexes often have several intense low-energy transitions. For reference, the relative contributions from the low-energy transitions to the maximum TPA, which are evaluated with the expression (3), are summarized in Table 4.

The Schiff base ligand **L** does not experimentally exhibit any two-photon absorption at 890 nm [24], while the data in Table 3 show that there is the maximum TPA (980.1 GM) at 692.8 nm for **L**. When metal cation is coordinated with the Schiff base ligand **L**, two-photon absorption is red-shifted (see peak I in Fig. 5) and TPA cross-section is significantly enhanced. At 606.0 nm and 625.2 nm, the dipole molecules **1-Cu** and **1-Zn** exhibit the maximum TPA cross-sections 3047.0 GM and 3522.0 GM, respectively. Compared with the dipolar complexes **1-Cu** and **1-Zn**, the maximum TPAs of the octupolar

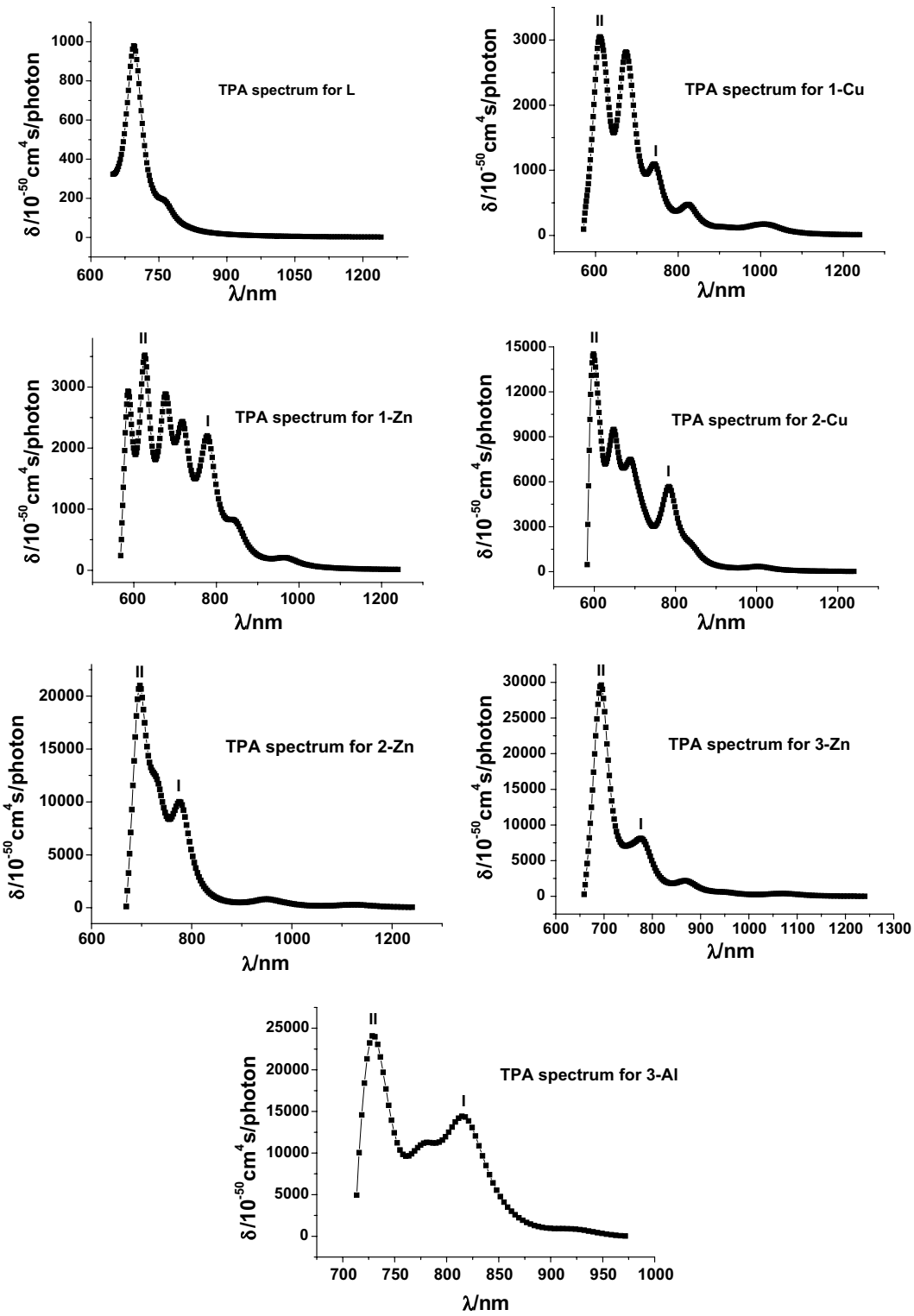

Fig. 5. Theoretically calculated TPA spectra of studied molecules.

tetrahedral complexes **2-Cu** and **2-Zn** are red-shifted 42.4 nm and 69.8 nm, respectively, the corresponding TPA cross-sections are increased by 6441.8 GM and 17470.9 GM, respectively. Comparing the TPA properties of two tetrahedral complexes **2-Cu** and **2-Zn**, it is found that the maximum TPA wavelength of **2-Zn** is red-shifted by 46.6 nm relative to **2-Cu** (648.4 nm for **2-Cu** and 695.0 nm for **2-Zn**, respectively), and at the same time, the maximum TPA is significantly enhanced on going from 9488.8 GM for **2-Cu** to 20992.9 GM for **2-Zn**. This is because that the stronger Lewis acidity of Zn(II) than Cu(I) leads to a larger scope of the electron delocalization

Table 3
Two-photon absorption properties of the investigated molecules and the available experimental values (in the parentheses)

Mol.	Transitions	λ^T_{max}(nm)	$\mathrm{Im}\,\gamma \times 10^{-36}$ (esu)	δ_{max} (GM)
L	$S_0 \rightarrow S_7$	692.8	6836.4	980.1
1-Cu	$S_0 \rightarrow S_5$	745.0	8733.1	1097.3
	$S_0 \rightarrow S_{15}$	606.0	16418.9	3047.0
1-Zn	$S_0 \rightarrow S_3$	779.4	19286.3	2202.5 (1769)[a]
	$S_0 \rightarrow S_9$	625.2	20028.5	3522.0
2-Cu	$S_0 \rightarrow S_{11}$	782.4	50516.3	5682.4
	$S_0 \rightarrow S_{28}$	648.4	57749.7	9488.8 (10198)[a]
2-Zn	$S_0 \rightarrow S_8$	778.2	87042.4	10015.2 (10736)[a]
	$S_0 \rightarrow S_{20}$	695.0	147416.2	20992.9
3-Zn	$S_0 \rightarrow S_{13}$	778.0	70409.0	8101.3
	$S_0 \rightarrow S_{31}$	694.0	206529.2	29609.6
3-Al	$S_0 \rightarrow S_{17}$	816.4	138600.1	14430.5
	$S_0 \rightarrow S_{31(32)}$	727.2	184959.6	24081.5

[a] Measured in dichloromethane solvent at 890 nm, Ref. [24].

Table 4
Contributions from low-energy transitions to peaks I and II (evaluated with three-state formula)

Mol.	$S_0 \rightarrow S_k$	$\lvert M_{0k}\rvert$(D)	$\lvert M_{kn}\rvert$ (D)		E_{0k} (eV)	E_{0n} (eV)		$\frac{M^2_{0k}M^2_{kn}}{(E_{0k}-E_{0n}/2)^2\Gamma}$	
			I	II		I	II	I	II
L	$S_0 \rightarrow S_1$	8.58	5.43		3.03	3.58		14116.6	
	$S_0 \rightarrow S_2$	6.71	3.64		3.24			2837.3	
1-Cu	$S_0 \rightarrow S_1$	7.01	1.2	3.54	2.42	3.33	4.09	1241.4	43790.5
	$S_0 \rightarrow S_3$	8.04	6.10	0.06	2.71			22026.2	5.3
	$S_0 \rightarrow S_4$	9.55	2.16	0.65	3.00			2387.5	422.5
1-Zn	$S_0 \rightarrow S_1$	10.98	8.90	5.57	2.56	3.18	3.96	101494.2	111188.3
	$S_0 \rightarrow S_2$	9.99	2.29	3.13	2.93			2914.7	10833.6
2-Cu	$S_0 \rightarrow S_1$	12.06	0.07	2.44	2.46	3.17	3.82	9.3	28625.2
	$S_0 \rightarrow S_2$	12.06	0.07	2.44	2.46			9.3	28625.2
	$S_0 \rightarrow S_5$	10.71	5.86	4.22	2.75			29021.7	28949.8
2-Zn	$S_0 \rightarrow S_1$	12.89	4.83	4.53	2.20	3.18	3.57	104169.5	197973.0
	$S_0 \rightarrow S_2$	12.89	4.83	4.53	2.20			104169.5	197973.0
	$S_0 \rightarrow S_3$	14.44	1.36	3.68	2.52			4459.1	52270.3
3-Zn	$S_0 \rightarrow S_1$	9.56	1.50	3.47	2.31	3.19	3.57	4022.4	39926.0
	$S_0 \rightarrow S_2$	9.56	1.50	3.47	2.31			4022.4	39926.0
	$S_0 \rightarrow S_3$	17.77	4.43	6.31	2.39			98050.1	343496.9
	$S_0 \rightarrow S_4$	10.11	0.49	3.29	2.60			242.9	16656.3
	$S_0 \rightarrow S_5$	10.11	0.49	3.29	2.60			242.9	16656.3
3-Al	$S_0 \rightarrow S_1$	10.95	2.63	0.43	2.04	3.04	3.41	30671.3	1975.5
	$S_0 \rightarrow S_2$	10.95	2.63	0.43	2.04			30671.3	1975.5
	$S_0 \rightarrow S_3$	20.04	5.45	1.53	2.13			320574.0	52047.6
	$S_0 \rightarrow S_4$	9.05	0.83	1.01	2.28			976.8	2527.0
	$S_0 \rightarrow S_5$	9.05	0.83	1.01	2.28			976.8	2527.0

in **2-Zn** than that in **2-Cu**. Compared with the **2-Cu** complex, the complex **2-Zn** is a better TPA material from the large TPA response point of view.

The octupolar complexes **2-Zn**, **3-Zn** and **3-Al** all exhibit two TPA peaks (the peak I and peak II in Fig. 5). Comparing the TPA properties of **2-Zn** and **3-Zn**, it is found that the positions of the peaks I and II for **2-Zn** and **3-Zn** are nearly the same (778 nm for peak I and 694 nm for peak II), respectively. This is different from the Zn(II) bipyridine complexes, in which the maximum TPA position is greatly blue-shifted from 968 nm for the tetrahedral Zn(II) complex to 827 nm for the octahedral Zn(II) complex [32]. This difference is due to the weaker spiroconjugation effect in the complex **2-Zn** than that in the tetrahedral Zn(II) bipyridine complex. Though the peak I value is slightly reduced from 10015.2 for **2-Zn** to 8101.3 GM for **3-Zn**, the value of peak II is significantly enhanced from 20992.9 GM for **2-Zn** to 29609.6 GM for **3-Zn**, due to the increased ligands

in **3-Zn**. When the Zn(II) center in **3-Zn** is replaced by Al(III), the value of peak I of **3-Al** (14430.5 GM) is enhanced relative to **3-Zn** (8101.3 GM), however, the value of peak II is decreased (29609.6 GM for **3-Zn** and 24081.5 GM for **3-Al**). Furthermore, the positions of peak I and peak II are red-shifted (778 nm and 694 nm for **3-Zn** vs. 816 nm and 727 nm for **3-Al**, respectively) due to the stronger Lewis acidity of Al(III) than Zn(II). From the large TPA response point of view, the octupolar octahedral complexes **3-Zn** and **3-Al** are better candidates for TPA material.

4. Conclusion

In this paper, one- and two-photon absorption properties for a series of octupolar complexes with the Cu(I), Zn(II) and Al(III) as center and the bis-cinnamaldimine as ligands have been theoretically studied. Firstly, their equilibrium geometries and electronic structures are obtained by the B3LYP density functional combined with 6-31G(d) basis set. Then, based on the correct geometries, their one- and two-photon absorption properties are calculated with the ZINDO-SOS method. Our calculated results show that compared with the dipolar metal complexes, the TPA cross-sections of the octupolar metal complexes are significantly enhanced. The Lewis acidity of metal cation and the molecular symmetry are two important factors for enhancement of TPA cross-section of octupolar metal complex. In the tetrahedral complex **2-Cu**, there are both the MLCT and ILCT during the electron excitation from the HOMO to LUMO, while in complex **2-Zn**, there is only the ILCT. This leads to larger scope of electron delocalization in **2-Zn** than that in **2-Cu** and to the greatly enhanced TPA cross-sections of **2-Zn** relative to **2-Cu**. Compared with the tetrahedral complex **2-Zn**, due to increase of number of ligand, the one-photon absorption of the octahedral complex **3-Zn** is blue-shifted, and at the same time, the maximum TPA cross-section is significantly enhanced. Replacing Zn(II) in **3-Zn** by Al(III) leads to redshift of the maximum TPA and complex **3-Al** maintains the large TPA cross-section.

Acknowledgments

This work is supported by the National Nature Science Foundation of China and the Key Laboratory for Supramolecular Structure and Materials of Jilin University.

Appendix A. Supplementary material

Cartesian coordinates for studied compounds at the level of B3LYP/6-31G(d) are available on http://www.sciencedirect.com/. Supplementary data associated with this article can be found, in the online version, at doi:10.1016/j.jorganchem.2007.03.021.

References

[1] (a) J.D. Bhawalkar, G.S. He, P.N. Prasad, Rep. Prog. Phys. 59 (1996) 1041;
(b) G.S. He, C.-F. Zhao, J.D. Bhawalkar, P.N. Prasad, Appl. Phys. Lett. 67 (1995) 3703;
(c) C.-F. Zhao, G.S. He, J.D. Bhawalkar, C.K. Park, P.N. Prasad, Chem. Mater. 7 (1995) 1979.
[2] (a) P.A. Fleitz, R.A. Sutherland, F.P. Stroghendl, F.P. Larson, L.R. Dalton, SPIE Proc. 3472 (1998) 91;
(b) G.S. He, J.D. Bhawalkar, C.-F. Zhao, P.N. Prasad, Appl. Phys. Lett. 67 (1995) 2433;
(c) J.E. Ehrlich, X.-L. Wu, I.-Y.S. Lee, Z.-Y. Hu, H. Röeckel, S.R. Marder, J.W. Perry, Opt. Lett. 22 (1997) 1843.
[3] J.D. Bhawalkar, N.D. Kumar, C.-F. Zhao, P.N. Prasad, J. Clin. Laser Med. Surg. 15 (1997) 201.
[4] (a) S. Maruo, O. Nakamura, S. Kawata, Opt. Lett. 22 (1997) 132;
(b) B.H. Cumpston, S.P. Ananthavel, S. Barlow, D.L. Dyer, J.E. Erskine, A.A.J. Oin, H. Röckel, M. Rumi, X.L. Wu, S.R. Marder, J.W. Perry, Nature 398 (1999) 51;
(c) S. Kawata, H.-B. Sun, T. Tanaka, K. Takada, Nature 412 (2001) 697;
(d) S. Maruo, K. Ikuta, Proc. SPIE-Int. Soc. Opt. Eng. 3937 (2000) 106.
[5] M. Albota, D. Beljonne, J.-L. Brédas, J.E. Ehrlich, J.-Y. Fu, A.A. Heikal, S.E. Hess, T. Kogej, M.D. Levin, S.R. Marder, D. McCord-Maughon, J.W. Perry, H. Röckel, M. Rumi, G. Subramaniam, W.W. Webb, X.-L. Wu, C. Xu, Science 281 (1998) 1653.
[6] (a) B. Reinhardt, L.L. Brott, S.J. Clarson, A.G. Dillard, J.C. Bhatt, R. Kannan, L. Yuan, G.S. He, P.N. Prasad, Chem. Mater. 10 (1998) 1863;
(b) R. Kannan, G.S. He, L. Yuan, F. Xu, P.N. Prasad, A. Dombroskie, B.A. Reinhardt, J.W. Baur, R.A. Vaia, L.-S. Tan, Chem. Mater. 13 (2001) 1896;
(c) C.-K. Wang, P. Macak, Y. Luo, H. Agren, J. Chem. Phys. 114 (2001) 9813.
[7] (a) L. Ventelon, S. Charier, L. Moreaux, J. Mertz, M. Blanchard-Desce, Angew. Chem. 113 (2001) 2156;
(aa) L. Ventelon, S. Charier, L. Moreaux, J. Mertz, M. Blanchard-Desce, Angew. Chem., Int. Ed. 40 (2001) 2098;
(b) A. Abotto, L. Beverina, R. Nozio, A. Facchetti, C. Ferrante, G.A. Pagani, D. Pedron, R. Signorini, Org. Lett. 4 (2002) 1495;
(c) B. Strehmel, A.M. Sarker, H. Detert, ChemPhysChem 4 (2003) 249.
[8] (a) J.D. Bhawalkar, G.S. He, C.-K. Park, C.F. Zhao, G. Ruland, P.N. Prasad, Opt. Commun. 124 (1996) 33;
(b) G.S. He, L. Yuan, N. Cheng, J.D. Bhawalkar, P.N. Prasad, L.L. Brott, S.J. Clarson, B.A. Reinhardt, J. Opt. Soc. Am. B 14 (1997) 1079;
(c) G.S. He, L. Yuan, P.N. Prasad, A. Abotto, A. Facchetti, G.A. Pagani, Opt. Commun. 140 (1997) 49;
(d) A. Abotto, L. Beverina, R. Bozio, S. Bradamante, C. Ferrante, G.A. Pagani, R. Signorini, Adv. Mater. 12 (2000) 1963.
[9] (a) A. Painelli, L. Del Freo, F. Terenziani, Chem. Phys. Lett. 346 (2001) 470;
(b) R. Zalesny, W. Bartowiak, S. Styrcz, J. Leszczynski, J. Phys. Chem. A 106 (2002) 4032;
(c) H. Lei, Z.L. Huang, H.Z. Wang, X.J. Tang, L.Z. Wu, G.Y. Zhou, D. Wang, Y.B. Tian, Chem. Phys. Lett. 352 (2002) 240.
[10] T. Kogej, D. Beljonne, F. Meyers, J.W. Perry, S.R. Marder, J.-L. Brédas, Chem. Phys. Lett. 298 (1998) 1.
[11] (a) W.L. Peticolas, Annu. Rev. Phys. Chem. 18 (1976) 233;
(b) W.M. McClain, Acc. Chem. Res. 7 (1974) 129;
(c) R.R. Birge, B.M. Pierce, J. Chem. Phys. 70 (1979) 165.
[12] (a) I. Ledoux, J. Zyss, J. Siegel, J.-M. Lehn, Chem. Phys. Lett. 172 (1990) 440;
(b) J. Zyss, Nonlinear Opt. 1 (1991) 3;

(c) J. Zyss, J. Chem. Phys. 98 (1993) 6583;
(d) J. Zyss, C. Dhenaut, T. Chau Van, I. Ledoux, Chem. Phys. Lett. 206 (1993) 409;
(e) J. Zyss, I. Ledoux, Chem. Rev. 94 (1994) 77.
[13] D.M. Burland, Chem. Rev. 94 (1994) 1.
[14] (a) F.W. Vance, J.T. Hupp, J. Am. Chem. Soc. 121 (1999) 4047;
(b) O. Maury, H. Le Bozec, Acc. Chem. Res. 38 (2005) 691.
[15] I.G. Voigt-Martin, G. Li, A. Yakimanski, G. Schulz, J.J. Wolff, J. Am. Chem. Soc. 118 (1996) 12830.
[16] J.L. Bredas, F. Meyers, B.M. Pierce, J. Zyss, J. Am. Chem. Soc. 114 (1992) 4928.
[17] (a) B.R. Cho, M.J. Piao, K.H. Son, S.H. Lee, S.J. Yoon, S.-J. Jeon, M. Cho, Chem. Eur. J. 8 (2002) 3907;
(b) S. Vagin, M. Barthel, D. Dini, A. Michael, Inorg. Chem. 42 (2003) 2683.
[18] (a) S.K. Hurst, M.G. Humphrey, T. Isoshima, K. Wostyn, I. Asselberghs, K. Clays, A. Persoons, M. Samoc, B. Luther-Davices, Organometallics 21 (2002) 2024;
(b) G. Alcaraz, L. Euzenat, O. Mongin, C. Katan, I. Ledoux, J. Zyss, M. Blanchard-Desce, M. Vaultier, Chem. Commun. (2003) 2766;
(c) L. Porrès, O. Mongin, C. Katan, M. Charlot, T. Pons, J. Mertz, M. Blanchard-Desce, Org. Lett. 6 (2004) 47.
[19] (a) B.C. Cho, K.H. Son, S.H. Lee, Y.S. Song, Y.K. Lee, S.J. Jeon, J.H. Choi, H. Lee, M. Cho, J. Am. Chem. Soc. 123 (2001) 10039;
(b) P.C. Ray, J. Leszczynski, J. Phys. Chem. A 109 (2005) 6689;
(c) R. Kannan, G.S. He, T.C. Lin, P.N. Prasad, R.A. Vaia, L.-S. Tan, Chem. Mater. 16 (2004) 185.
[20] (a) S.-J. Chung, K.-S. Kim, T.C. Lin, G.S. He, J. Swiatkiewicz, P.N. Prasad, J. Phys. Chem. B 103 (1999) 10741;
(b) W.-H. Lee, H. Lee, J.-A. Kim, J.-H. Choi, M. Cho, S.-J. Jeon, B.R. Cho, J. Am. Chem. Soc. 123 (2001) 10658;
(c) D. Beljonne, E. Zojer, Z. Shuai, H. Vogel, W. Wenseleers, S.J.K. Pond, J.W. Perry, S.R. Marder, J.-L. Bredas, Adv. Funct. Mater. 12 (2002) 631;
(d) P. Macak, Y. Luo, P. Norman, H. Ågren, J. Chem. Phys. 113 (2000) 7055;
(e) S.J. Chung, T.C. Lin, K.S. Kim, G.S. He, J. Swiatkiewicz, P.N. Prasad, G.A. Baker, F.V. Bright, Chem. Mater. 13 (2001) 4071;
(f) H.J. Lee, J.W. Sohn, J.H. Hwang, S.Y. Park, Chem. Mater. 16 (2004) 456;
(g) X.-J. Liu, J.-K. Feng, A.-M. Ren, H. Cheng, X. Zhou, J. Chem. Phys. 121 (2004) 8253.
[21] (a) X. Zhou, J.-K. Feng, A.-M. Ren, Chem. Phys. Lett. 403 (2005) 7;
(b) G.P. Bartholomew, M. Rumi, S.J.K. Pond, J.W. Perry, S. Tretiak, G.C. Bazan, J. Am. Chem. Soc. 126 (2004) 11529;
(c) X.-B. Zhang, J.-K. Feng, A.-M. Ren, C.-C. Sun, J. Mol. Struct. (THEOCHEM) 756 (2005) 133;
(d) X. Zhou, A.-M. Ren, J.-K. Feng, X.-J. Liu, Chem. Phys. Lett. 373 (2003) 167;
(e) X.-B. Zhang, J.-K. Feng, A.-M. Ren, X. Zhou, Chem. Phys. 322 (2006) 269.
[22] S.J.K. Pond, O. Tsutsumi, M. Rumi, O. Kwon, E. Zojer, J.-L. Brédas, S.R. Marder, J.W. Perry, J. Am. Chem. Soc. 126 (2004) 9291.
[23] Q. Zheng, G.S. He, P.N.J. Prasad, J. Mater. Chem. 15 (2005) 579.
[24] S. Das, A. Nag, D. Goswami, P.K. Bharadwaj, J. Am. Chem. Soc. 128 (2006) 402.
[25] M. Cha, W.E. Torruellas, G.I. Stegeman, W.H.G. Horsthuis, G.R. Möhlmann, J. Meth, Appl. Phys. Lett. 65 (1994) 2648.
[26] T. Kogej, D. Beljoone, F. Meyers, J.W. Perry, S.R. Marder, J.-L. Brédas, Chem. Phys. Lett. 298 (1998) 1.
[27] B.J. Orr, J.F. Ward, Mol. Phys. 20 (1971) 513.
[28] D.M. Bishop, J.M. Luis, B. Kirtman, J. Chem. Phys. 116 (2002) 9729.
[29] M.J. Frisch et al., GAUSSIAN 03, Revision C.02, Gaussian, Inc., Wallingford, CT, 2004.
[30] W.P. Anderson, W.D. Edwards, M.C. Zerner, Inorg. Chem. 25 (1986) 2728.
[31] (a) R. Hoffmann, A. Imamura, G.D. Zeiss, J. Am. Chem. Soc. 89 (1967) 5215;
(b) H.E. Simmons, T. Fukunaga, J. Am. Chem. Soc. 89 (1967) 5208;
(c) J.K. Feng, X.Y. Sun, A.M. Ren, K.Q. Yu, C.C. Sun, J. Mol. Struct. (THEOCHEM) 487 (1999) 247;
(d) W. Fu, J.K. Feng, G.B. Pan, X. Zhang, Theor. Chem. Acc. 106 (2001) 241.
[32] X.-J. Liu, J.-K. Feng, A.M. Ren, H. Cheng, X. Zhou, J. Chem. Phys. 120 (2004) 11493.
[33] E. Zojer, T. Kogej, H. Vogel, S.R. Marder, J.W. Perry, J.L. Brédas, J. Chem. Phys. 116 (2002) 3646.